



HAL
open science

A holistic NMR framework to understand environmental impact: Examining the impacts of superparamagnetic iron oxide nanoparticles (SPIONs) in *Daphnia magna* via imaging, spectroscopy, and metabolomics

Amy Jenne, Ronald Soong, Oliver Gruschke, Monica Bastawrous, Patricia Monks, Cara Moloney, Dermot F. Brougham, Falko Busse, Wolfgang Bermel, Denis Courtier-Murias, et al.

► To cite this version:

Amy Jenne, Ronald Soong, Oliver Gruschke, Monica Bastawrous, Patricia Monks, et al.. A holistic NMR framework to understand environmental impact: Examining the impacts of superparamagnetic iron oxide nanoparticles (SPIONs) in *Daphnia magna* via imaging, spectroscopy, and metabolomics. *Magnetic Resonance in Chemistry*, 2023, 17p. 10.1002/mrc.5315 . hal-04042883

HAL Id: hal-04042883

<https://hal.science/hal-04042883v1>

Submitted on 23 Mar 2023

HAL is a multi-disciplinary open access archive for the deposit and dissemination of scientific research documents, whether they are published or not. The documents may come from teaching and research institutions in France or abroad, or from public or private research centers.

L'archive ouverte pluridisciplinaire **HAL**, est destinée au dépôt et à la diffusion de documents scientifiques de niveau recherche, publiés ou non, émanant des établissements d'enseignement et de recherche français ou étrangers, des laboratoires publics ou privés.



A holistic NMR framework to understand environmental impact: Examining the impacts of superparamagnetic iron oxide nanoparticles (SPIONs) in *Daphnia magna* via imaging, spectroscopy, and metabolomics

Journal:	<i>Magnetic Resonance in Chemistry</i>
Manuscript ID	MRC-22-0065
Wiley - Manuscript type:	Special Issue Research Article
Date Submitted by the Author:	11-Aug-2022
Complete List of Authors:	Jenne, Amy; University of Toronto at Scarborough, Chemistry Soong, Ronald; University of Toronto at Scarborough, Chemistry Gruschke, Oliver; Bruker BioSpin MRI GmbH Bastawrous, Monica; University of Toronto at Scarborough, Physical and Environmental Science Monks, Patricia; RCSI University of Medicine and Health Sciences Moloney, Cara; University of Nottingham Brougham, Dermot; University College Dublin Busse, Falko; Bruker BioSpin GmbH Bermel, Wolfgang Courtier-Murias, Denis; IFSTTAR Nantes, Department of Geotechnology Environment Natural Hazards and Earth Sciences Wu, Bing; University of Toronto at Scarborough, Chemistry Simpson, Andre; University of Toronto at Scarborough, Chemistry
Keywords:	NMR, MRI, ¹ H, ¹³ C, in-vivo, metabolomics, sub-lethal toxicity, environmental, superparamagnetic, iron oxide nanoparticles

SCHOLARONE™
Manuscripts

A holistic NMR framework to understand environmental impact: Examining the impacts of superparamagnetic iron oxide nanoparticles (SPIONs) in *Daphnia magna* via imaging, spectroscopy, and metabolomics

Amy Jenne,¹ Ronald Soong,¹ Oliver Gruschke,² Monica Bastawrous,¹ Patricia Monks,³ Cara Moloney,⁴ Dermot F. Brougham,⁵ Falko Busse,² Wolfgang Bermel,² Denis Courtier-Murias^{6,7} Bing Wu,^{8*} and Andre Simpson^{1*}

¹Environmental NMR Center, University of Toronto Scarborough, 1265 Military Trail, Scarborough, Ontario, Canada, M1C1A4

²Bruker BioSpin GmbH, Rudolf-Plank-St. 23, 76275, Ettlingen, Germany

³Department of Chemistry, RCSI University of Health Sciences, 123 St. Stephen's Green, Dublin 2, Ireland

⁴School of Medicine, BioDiscovery Institute-3, University of Nottingham, University Park, Nottingham NG7 2RD, UK

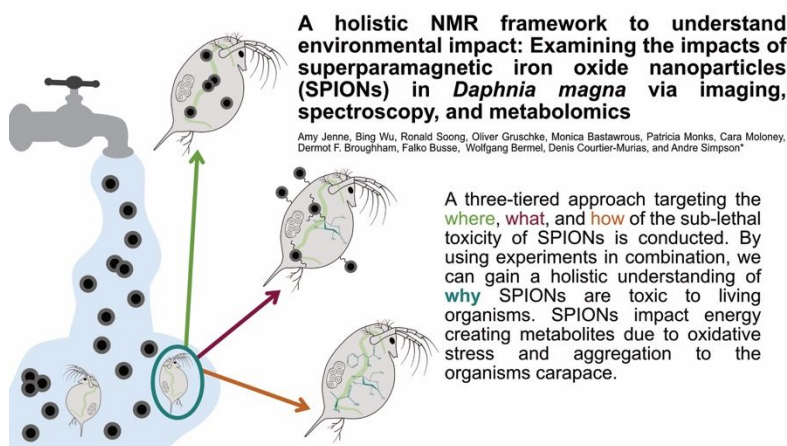
⁵School of Chemistry, University College Dublin, Belfield, Dublin 4, Ireland

⁶Univ Gustave Eiffel, GERS-LEE, F-44344 Bouguenais, France

⁷Institut de Recherche en Sciences et Techniques de la Ville IRSTV, CNRS, 1 rue de la Noë, 44321 Nantes Cedex 3, France

⁸Institute for Molecules and Materials, Radboud University, Heyendaalseweg 135, 6525 AJ Nijmegen, The Netherlands

*Corresponding Author: andre.simpson@utoronto.ca, friedrichbing.wu@utoronto.ca@utoronto.ca



Abstract

Superparamagnetic Iron Oxide Nanoparticles (SPIONs) are a contaminant of emerging interest, often used in the medical field as an imaging contrast agent, with additional uses in wastewater treatment and as food additives. While the use of SPIONs is increasing, little research has been conducted on the toxic impacts to living organisms beyond traditional lethal concentration endpoints. *Daphnia magna* are model organisms for aquatic toxicity testing with a well understood metabolome and high sensitivity to SPIONs. Thus, as environmental concentrations continue to increase, it is becoming critical to understand their sub-lethal toxicity. Due to the paramagnetic nature of SPIONs, a range of potential Nuclear Magnetic Resonance Spectroscopy (NMR) experiments are possible, offering the potential to probe the physical location (via imaging), binding (via relaxation weighted spectroscopy), as well as the biochemical pathways impacted (via *in-vivo* metabolomics). Results indicate binding to carbohydrates, likely chitin in

1
2
3 the exoskeleton, along with a decrease in energy metabolites and specific biomarkers of oxidative
4 stress. The holistic NMR framework used here helps provide a more comprehensive
5 understanding of SPIONs impacts on *Daphnia magna*, and showcases NMR's versatility in
6 providing physical, chemical and biochemical insights.
7
8

9 **Keywords**

10 NMR, MRI, ^1H , ^{13}C , *in-vivo*, metabolomics, sub-lethal toxicity, environmental, superparamagnetic,
11 iron oxide nanoparticles
12
13

14 **Introduction**

15 Nanomaterials have become an increasingly prevalent substance used in numerous applications
16 from food additives to preservatives, as well as in medicine and wastewater treatment, and
17 production only continues to expand.^[1-4] In the last decade there has been a 25-fold increase in
18 products which used nanoparticles during their production.^[3] However, despite their increased
19 use, little research has been performed as to their environmental impact. Due to their small size,
20 nanoparticles can move through the environment with ease and as many nanoparticles are
21 metal-based, the potential ramifications to the biotic environment can be severe.^[2]
22 Superparamagnetic Iron Oxide Nanoparticles (SPIONs) are one such potential contaminant
23 where impacts to the environment are not fully understood. The most common use of SPIONs is
24 in the medical field as clinical Magnetic Resonance Imaging (MRI) contrast agents. The presence
25 of SPIONs alters the surrounding water molecules spin-spin relaxation in particular, causing them
26 to relax faster and resulting in local suppression of image intensity (darkening) under T_2 -weighted
27 imaging conditions.^[5] This is particularly useful in disease monitoring as the suppression is
28 proportional to the concentration of particles.^[6] When surface functionalized with appropriate
29 ligands, SPIONs can be selectively consumed by cancer cells, helping identify tumorous regions,^[7]
30 passive targeting is also well documented.
31
32
33
34
35

36 For human consumption, SPIONs are coated in a stable ligand, thus considered non-toxic. As a
37 result, SPIONs move through the body based on their half-life (proportional to their size) and
38 then are passed through the liver and are eventually eliminated as waste.^[5,7,8] However, there
39 has been limited research examining the toxicity of released particles to aquatic life, particularly
40 from sub-lethal or mechanistic perspectives. Nanoparticles released by the body end up in
41 wastewater, and as they enter our freshwater systems, they can be consumed by primary
42 consumers such as *Daphnia magna*. *D. magna* are one of the most utilized model organisms in
43 environmental toxicity testing and multiple studies have measured the impacts of other types of
44 nanoparticles such as silver, titanium, and silicon oxide particles.^[9-11] However, to date,
45 metabolomic studies with iron oxide nanoparticles are lacking. The limited research that has
46 been conducted on the toxic impacts of SPIONs have focused on apical endpoints with respect to
47 lethal concentrations, rather than a mechanistic understanding. *Daphnia magna* have been
48 shown to be incredibly susceptible to SPIONs, with an LC_{50} of 2.3×10^{-4} mg/mL.^[12] However,
49 information targeting the "where, what, how, and why" of SPION toxicity is still lacking.
50
51
52
53

54 Magnetic resonance imaging and spectroscopy when used in combination have a unique ability
55 to provide comprehensive insights into the issue. As the contaminant is a contrast agent MRI has
56
57
58
59
60

potential to show within *Daphnia magna* physically “where” SPIONs accumulate, while also providing average or localized changes in relaxation. Hence relaxation measurements are useful when evaluating how effectively different size SPIONs are consumed. This is especially important as *Daphnia* are filter feeders, and little is known about the minimum size of particles they can consume or how specific ligand coatings may impact uptake. Another consideration is determining whether the nanoparticles are consumed at all, or if the toxic response is only as a result of the interactions with the outside of the organism.^[9–11] If they are ingested, then “what” the nanoparticles bind with inside the organism at the molecular level must be examined. Here, relaxation filtered 2D NMR spectroscopy could be useful to study the categories of molecules or even structures that bind to SPIONs, aiding in understanding their excretion or bioaccumulation.^[13,14] Finally, the question as to “how” the SPIONs are toxic can be tackled using *in-vivo* NMR metabolomics. This is the measurement of changes to an organism’s metabolome as a result of an external stressor.^[15] Sub-lethal toxicity in *Daphnia magna* has been assessed in this way, however utilizing *in-vivo* NMR spectroscopy is particularly desirable, as changes to the organism’s metabolome can be measured in close to real time.^[16–22] To the authors knowledge, to date there have been no studies of nanoparticles *in-vivo*. Perturbations to specific metabolic pathways could provide important information on the toxicity of SPIONs and help explain the toxic-mode-of-action inside *Daphnia magna*, as an exemplar aquatic organism, which are essential for setting updated environmental policies.

In this study, a-proof-of-concept study is presented that combines imaging, relaxation filtered 2D NMR, and *in-vivo* metabolomics to provide a more comprehensive overview addressing the “why” of SPION fate and toxicity. Given magnetic resonance’s ability to provide detailed molecular information in a non-invasive fashion, such unified approaches drawing from different branches of NMR/MRI are shown to provide holistic understanding of the complex physiochemical processes in SPION toxicity, that may prove generally translatable.

Materials and Methods

Unless otherwise stated, all chemicals were purchased from Sigma Aldrich (St. Louis, Missouri, U.S).

SPION Synthesis and Validation Measurements

Preparation of Primary Nanoparticles

4 nm (core size) primary SPIONs were prepared with slight modifications to the Pinna method.^[23] In brief, 20 mL of 141.6 mM Fe(acac)₃ in benzyl alcohol was purged with N₂ for 20 minutes and refluxed at 205°C for 7 hours. The resulting black solution contained 10 mg/mL γ-Fe₂O₃ (90% yield) of 8.6 nm SPIONs as determined by transmission electron microscopy (TEM). To prepare the 12 nm SPIONs used in this study, 20 mL of 8.6 nm SPIONs were washed twice with benzyl alcohol and resuspended in 20 mL of 141.6 mM Fe(acac)₃ in benzyl alcohol. The solution was purged with N₂ for 20 minutes and refluxed at 205°C for 7 hours. The resulting black solution contained 20 mg/mL γ-Fe₂O₃ (90% yield) of 12 nm SPIONs as determined by TEM. SPIONs were stored under N₂ until use to prevent oxidation.

Stabilization of Primary Nanoparticles

1
2
3 5 mL of nanoparticles were washed twice with acetone using a magnetic separator. 37 μL of
4 GLYMO in 2 mL THF was added to the wet nanoparticles and tumbled for 24 h. 10 μL of
5 hydrochloric acid (1 M) and ethanol were also added to catalyze the hydrolysis and condensation
6 of the alkoxy silane groups. This process yields a stable dispersion of GLYMO-functionalized Fe_3O_4
7 nanoparticles. PEG-NH₂ (of different M_n) in THF was added to the SPIONs in a 10:1
8 polymer:GLYMO ratio. Following the addition of 50 μL KOH (1 M), the PEG-grafted SPIONs
9 precipitated out, were washed with THF and redispersed in water. The procedure has previously
10 been reported.^[24]
11
12
13

14 TEM

15 Transmission electron microscopy was performed on a FEI Tecai G2 TWIN 200 kV microscope.
16 Aqueous suspensions of SPIONs were prepared (concentrations of 5 mM Fe) and 5 μL was
17 pipetted onto a carbon TEM grid (Formvar and carbon films on 400 μm copper grid, Agra
18 Scientific). Size analysis was performed using ImageJ software.
19
20

21 DLS

22 Dynamic light scattering (DLS) measurements were performed using a Malvern Nano ZetaSizer
23 (Malvern Instruments, Malvern UK). A 3 mW He-Ne laser operating at a wavelength of 633 nm
24 was used and back scattered light is detected at an angle of 173° to the incident beam. Data was
25 processed using Dispersion technology software (v 7.13, Malvern instruments, Malvern UK) using
26 the multiple narrow modes algorithm based upon a non-negative least square fit to calculate the
27 hydrodynamic diameter (d_{hyd}) and the polydispersity Index (PDI). Samples were diluted to 5 mM
28 Fe and analysis was performed at 25 °C, with a thermal equilibration time of 30 seconds prior to
29 measurement.
30
31
32
33

34 Daphnia magna Culturing

35 *D. magna* were cultured from a colony originally purchased from Ward's Scientific but have been
36 maintained in the lab since 2017. Organisms were cultured at 20°C, a water hardness of 124 mg/L
37 CaCO_3 , and pH 7.5-8.5, consistent with local freshwater conditions. Cultures were kept under a
38 16:8 light/dark cycle and a 40% water media exchange occurred three times per week. For *in/ex-*
39 *vivo* experiments, species were cultured on a diet of 99% ¹³C enriched *Chlamydomonas*
40 *reinhardtii* (purchased from Silantes, GmbH)^[25] as their sole food source from birth. Prior to
41 experiments, organisms were placed in fresh dechlorinated water to clear off residual algae and
42 fed ¹²C algae to clear their gut, meaning only signals from the *Daphnia* would be measured.
43 During *in-vivo* experiments, organisms were continuously fed unenriched *Chlamydomonas*
44 *reinhardtii* cultured in the lab. Adult *Daphnia magna* (~two weeks old) born from ¹³C enriched
45 parents, are used in the study which have been shown to be ~99% ¹³C enriched.^[26,27] For imaging
46 experiments, organisms were not isotopically enriched, but other culturing parameters remained
47 the same.
48
49
50
51

52 Nanoparticle Exposure

53 In *Daphnia* samples used for *ex-vivo* exposure, 250 mL beakers were filled with 100 mL of
54 culturing media (as above), 10 adult *Daphnia magna* were added to each beaker and
55 nanoparticles were dosed in at a volume creating a total concentration of 10% of the LC₅₀ (2.3 x
56
57
58
59
60

1
2
3 10⁻⁵ mg/mL).^[12] Organisms were exposed for 48 hours and fed halfway through exposure to
4 ensure a lack of stress response from starvation. Once completed, organisms were removed from
5 exposure vessels and placed in beakers with clean media to allow any aggregated nanoparticles
6 on the outside of their bodies to be washed. These were then prepared for the imaging and T₁
7 weighted spectroscopy. Note for the *in-vivo* metabolomics, the organisms were exposed inside
8 the NMR as described below.
9
10

11 Imaging *Daphnia magna* Experiments

12 Immediately prior to experiments, *Daphnia magna*, one from control cultures and one from
13 exposed, were placed in a 2.5 mm glass NMR tube, cut to the size of the imaging probe.
14 Organisms were alive when they were placed in the tube and suspended in Fomblin (Solvay
15 Fomblin® Y, LVAC 06/6, average mol wt. 1800), but died once immersed in the oil. Note, Fomblin
16 is a perfluorinated oil and contributes no ¹H signal. In each tube there was a single control and
17 exposed *Daphnia* to measure the differences in the contrast through proton imaging.
18 Experiments were run in triplicate for each ligand size (3 SPION samples, 9 samples total).
19
20
21

22 Ex-vivo *Daphnia magna* – T₁ Weighted Spectroscopy

23 360 fully grown *Daphnia magna* were removed from the culture (180 from the control culture,
24 180 from the nanoparticles exposure), immediately frozen with liquid nitrogen to halt metabolite
25 response, and lyophilized. 30 minutes prior to experimentation 60 freeze-dried organisms (from
26 either control or exposed samples) were placed in a 5 mm NMR tube and re-swollen with 600 μL
27 of 90% H₂O/10% D₂O with 0.5% W/W sodium azide to prevent bacterial growth. Organisms were
28 kept intact and analyzed at 5°C inside the NMR to prevent degradation. Experiments were
29 conducted in triplicate.
30
31
32

33 In-vivo *Daphnia magna* – Metabolomics

34 Immediately prior to experiments, 30 *Daphnia magna* from standard cultures (not yet exposed
35 to nanoparticles) were transferred into a specially designed low-flow *in-vivo* flow system
36 (including an external lock capillary isolated from the organisms), as previously described.^[22] The
37 water reservoir contained the same media as the culture, and algae concentrations were
38 maintained for the duration of the exposure to ensure no starvation responses. The sample was
39 kept at 5°C for the experiment.^[19] After 6 hours, SPIONS were added to the flow system to create
40 a total concentration the same as that used above (10% of the LC₅₀). Organisms were monitored
41 for a total of 24 hours. Control experiments were also conducted for a full 24 hours maintaining
42 the flow to show differences between exposed and non-exposed organisms.
43
44
45
46

47 **Experimental Parameters**

48 Unless otherwise stated, all experiments were performed at 278 K using a Bruker Avance III HD
49 NMR 500 MHz spectrometer, fitted with a 5 mm ¹³C-¹⁵N TCI Prodigy cryoprobe fitted with an
50 actively shielded Z-gradient.
51
52

53 Imaging

54 ¹H 2D/3D NMR imaging measurements were performed on a Bruker Avance III HD 500 MHz
55 spectrometer equipped with Bruker micro-imaging accessory including a GREAT-60 amplifier and
56
57
58
59
60

a Bruker DIFF50 probe with a Z-gradient of 28.5 T m⁻¹ maximum (at Bruker, Rheinstetten/Germany). For 3D microimaging acquisition with T₂-weighting, a multi-slice spin-echo sequence (MSME) was used with a repetition time (TR) of 0.5 s, an echo time (TE) of 4 ms and 16 average (NA). For T₂ analyses, a MSME-based protocol (Bruker MSME-T₂-map) was used with a resolution of 0.1 mm × 0.1 mm. All images were collected with Bruker ParaVision 6.0.1.

T₁ Weighted Spectroscopy

A pseudo 3D ¹H-¹³C HSQC correlation via double inept transfer using an Echo/Antiecho-TPPI gradient, for selection and sensitivity improvement. Data were collected with 96 increments, 24 scans, at 12 different T₁'s (from 0 – 2.0 s). The T₁ delay was applied with ¹³C magnetization along Z, while a train of 180° ¹H pulses was applied to refocus H-C couplings. Experiments were collected with 2048-time domain points, a recycle delay of 5.0 s, ¹J_{CH} of 145 Hz, an adiabatic shape pulse for inversion (500 μs, Crp60,0.5,20.1), and an adiabatic shape pulse for refocusing (2 ms, Crp60comp.4). The 90° pulses were determined for each sample. Data were processed with a sine-squared function phase shifted by 90° in both dimensions and a zero-filling factor of 2. Fitting was performed in Bruker Protein Dynamic Center to extract the T₁ relaxation times. The 3D T₁ heat map (Figure 5) was generated using Python 3.0 via Thonny based on the percent changes of the T₁ relative to the controls. The code can be found in the supplementary materials. Briefly, a 3D gaussian shape was used to generate the peak shape for each T₁ value where the width of the gaussian was adjusted to match that of the ¹H-¹³C HSQC.

In-vivo NMR Experiments

A phase sensitive ¹H-¹³C HSQC using Echo/Antiecho-TPPI gradient selection was run using a total of 128 increments, each with 52 scans, 2048-time domain points, a recycle delay of 1.0 s, ¹J_{CH} of 145 Hz, and an adiabatic shape pulse for inversion (500 μs, Crp60,0.5,20.1). 90° pulses were determined for each sample. Data were processed with a sine-squared function phase shifted by 90° in both dimensions and a zero-filling factor of 2.

Spectral Assignments

Compound identification and assignment was completed using AMIX (Analysis of MIXtures software package, version 3.9.15, Bruker BioSpin, in combination with the Bruker Bio-reference NMR databases version 2-0-0 through 2-0-5). Spectra were calibrated against the Bruker Bio-reference NMR databases using tyrosine and D-glucose resonances as reference peaks. Assignments were performed using a procedure previously described.^[28,29] Relative changes in metabolites during *in-vivo* exposure were found using MestReNova 14.1.0 using spectral stacks and the peaks graphs resulting from global spectral deconvolution.

Results and Discussion

Nanoparticle Size

Daphnia magna are filter feeding organisms. As they move through water, food (or particulate matter) is taken in and must pass through a filter before being ingested.^[30,31] Only if the particles are the correct size, will they proceed into the gut.^[31] If a particle is too large they will be removed by the *Daphnia* furcal claws, while particles that are too small pass through without interacting with the organism.^[30] Previous studies have shown 0.5 μm particles result in the highest uptake

by *Daphnia magna*, but particles down to 0.1 μm have been measured.^[30] To our knowledge, no studies have examined uptake and accumulation in the lower nanometer range. However, the increased prevalence of nano-sized contaminants (micro/nano plastics and nanoparticles) support the need for more research in this area. In addition, acute toxicity tests have shown that SPIONs are toxic to *Daphnia*,^[12] yet the wide-spread implications and toxic mechanisms are not well understood.^[32,33]

To address this gap, nanoparticles of c.12 nm core size were synthesized with three different ligand shell sizes of polyethylene glycol (PEG): 1, 5, and 10 kDa. PEG has low cytotoxicity, is clinically approved for some applications, and it is one of the most used ligands with SPIONs. The highly hydrated and dynamic grafted ethyleneglycol chains can provide colloidal stabilization and dispersion of the particles in isotonic media at different pH.^[32] The chains also reduce protein binding *in-vivo*, which reduces uptake by macrophages in the human body.^[5,32] TEM and DLS measurements were undertaken, see Figure 1. The average core size, from TEM, is 12.4 nm and the average hydrodynamic size, from DLS, progressively increasing from ~16.5, to ~18.0 to ~19.1 nm, for 1, 5 and 10 kDa grafts respectively, and the polydispersity indices were low. Hence the difference in d_{hyd} arise from the chain length, which confirms full particle dispersion (absence of aggregates in suspension). This is important as we have shown that for fully dispersed particles the MRI contrast effect is unchanged for different graft types and lengths.^[34] *Daphnia magna* were then exposed to determine which size was most impactful in terms of consumption.

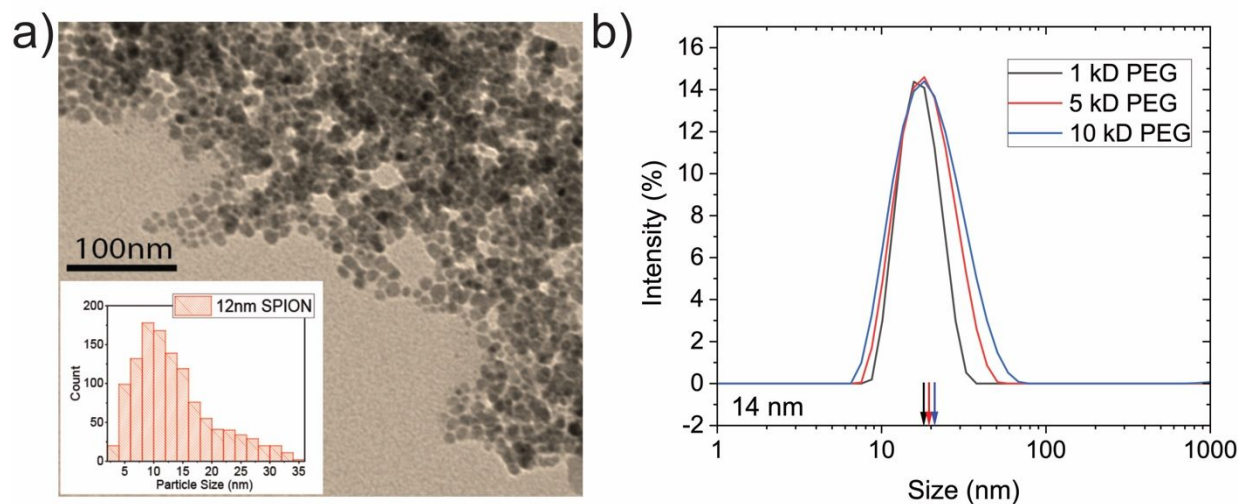
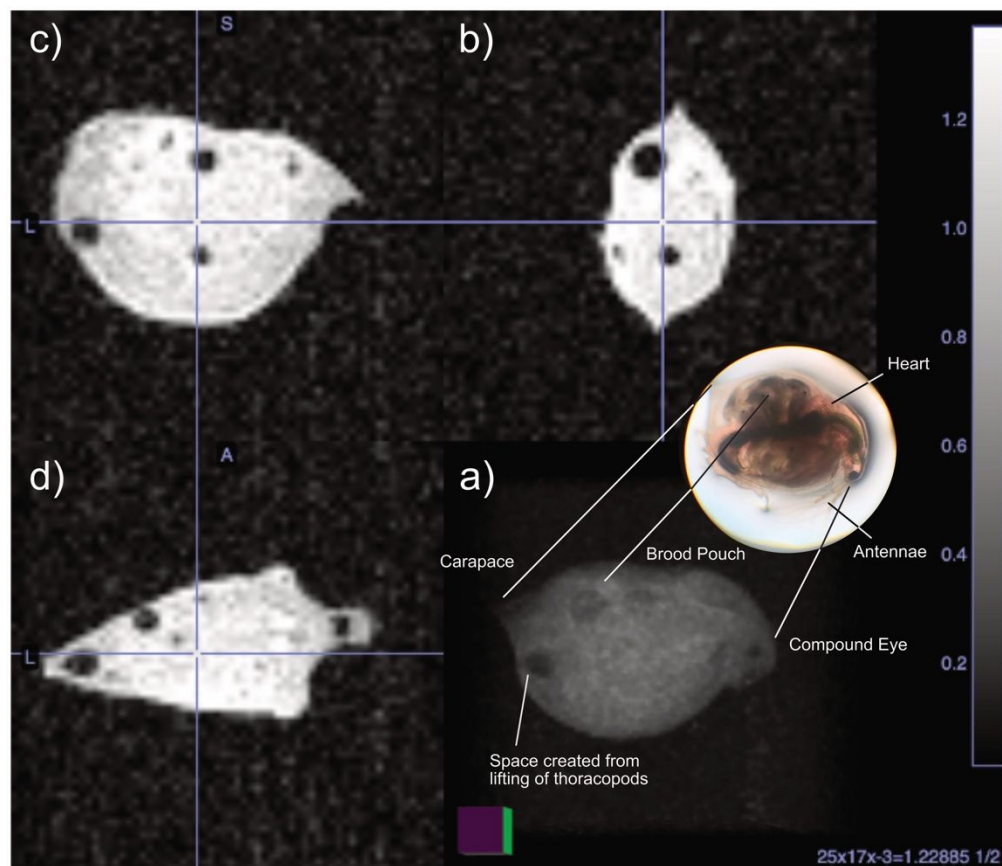


Figure 1. Confirmation of nanoparticle core and ligand size. a) Transmission electron microscopy (TEM) of the SPION cores to measure average sizing, determined to be 12.4 nm. b) Dynamic light scattering analyses of ligand (PEG)-stabilized SPION particle suspensions in H_2O . The average d_{hyd} size (core plus PEG ligands) progressively increases from 16.5 to 19.1 nm. The three suspensions were used to image *Daphnia magna* to determine the most impactful uptake based on the change in T_2 relaxation within the organism.

Imaging

In ^1H MRI, water inside the subject is imaged allowing for the visualization of different internal structures. One of the primary uses of SPIONs is in the medical field as an MRI contrast agent, resulting in localized darkening. To our knowledge, MR imaging of *Daphnia magna* has not yet

1
2
3 been reported. A 3D video with all the internal structures of a *Daphnia magna* is linked in the
4 supporting information file, while representative still images are shown in Figure 2 to provide an
5 overview of *Daphnia* physiology.
6
7



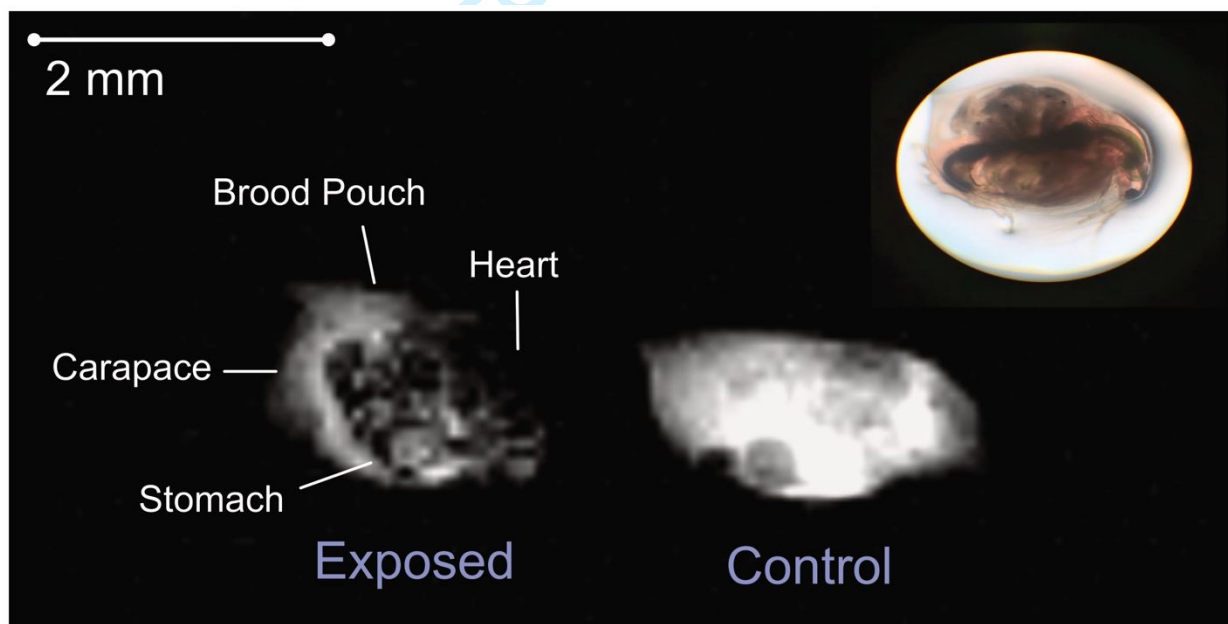
36
37
38
39
40
41
42
43
44
45
46
47
48
49
50
51

Figure 2. MRI of dead *Daphnia magna*. a) Standard spin echo image of a *Daphnia magna* with internal components labelled including compound eye, external carapace (uncalcified shell surrounding the *Daphnia*), and the spaces between the embryos inside the brood pouch. The dark space at the bottom of the *Daphnia magna* is a vacant spot due to the lifting of the thoracopods ('feet'). Note: the antennae labelled in the reference light microscope image would also be present in the MRI, but in this organism, it is tucked along the carapace rather than facing outwards. b-d) 2D sagittal, coronal, and axial planes extrapolated from the 3D image organism allowing for additional visualization of the labelled components in the 3D image.

52
53
54
55
56
57
58
59
60

Of more interest to this specific study is the impact of SPIONs on *Daphnia magna* images, which provide may insight as to "where" the SPIONs accumulate. Figure 3 shows an example of SPIONs inside *Daphnia magna*. On the right side is a control organism, while the left is one that has been

1
2
3 exposed to 10% of the LC_{50} of SPIONs for 48 hours prior to imaging.^[12] Note, the organisms were
4 washed to remove any nanoparticles interacting with the outside of the organism, allowing
5 internal uptake by the *Daphnia* to be better evaluated. SPIONs here are T_2 contrast agents,
6 meaning they reduce the relaxation time of the surrounding water, darkening the image where
7 they are localized. Thus, imaging can theoretically show where SPIONs accumulate internally in
8 the organism. Firstly, it can be confirmed that the washing was successful, and nanoparticles are
9 not simply stuck to the outside of the organism, as the image would have been completely dark
10 around all the edges (Figure 3). Additionally, considerable darkening is seen within the organism
11 interior, confirming nanoparticle uptake. Nanoparticles are clearly present in the stomach and
12 other internal compartments of the organism, but not the carapace (the outer exoskeleton of the
13 organism). There is also a lack of darkening in the brood pouch on top of the organism, indicating
14 the SPIONs had not yet accumulated in the eggs. Previous work examined the results of feeding
15 10 μm microbeads to *Daphnia*, in which they were contained strictly in the digestive track.^[35]
16 However, the widespread darkening here, especially the region around the heart, suggests the
17 SPIONs can access many of the organs following ingestion. In particular, the heart is not visible
18 at all. This suggests the SPIONs may be able to enter the hemolymph and thus may be transported
19 within the organism's circulatory system.
20
21
22
23
24



45
46
47
48
49
50
51
52
53

Figure 3. MRI of dead *Daphnia magna* using SPIONs as a T_2 contrast agent. The right represents an organism that was not exposed to SPIONs. The left represents a *Daphnia* which had been exposed to 10% of the LC_{50} for 48 hours prior to imaging. In the exposed organism the areas in proximity to the SPIONs are darkened. Darkening can be seen in the internal organs, stomach, and especially the heart. The regions least darkened are the carapace (the outer exoskeleton) and the brood pouch. In past studies nanoparticles have been seen to bind to the outside of the carapace, this has been reduced here via washing so that internal uptake is easier to discern.

54 While localization of the nanoparticles within the organism is difficult to assess given the size of
55 the animal, the average change in the T_2 relaxation caused by the SPIONs provide useful insights
56
57
58
59
60

into how the different ligand sizes impact *Daphnia* consumption. The changes in the organism averaged T_2 relaxation times are shown in Figure 4. The smallest size (1 kDa ligand) appears to have little impact on the T_2 relaxation indicating it was either too small for *Daphnia* to ingest, quickly passed through the digestive system, or sedimented from the suspension (due to the shorter chain length) and was not available for uptake. All suspensions were sonicated prior to dosing the *Daphnia* and the DLS analysis suggests no difference in the colloidal stability, so it is not clear what the cause is. In any case, of the two larger sizes, the 5 kDa ligand reduced the average relaxation time the most, consistent with it accumulating to the highest extent within the organisms. Ultimately, imaging provides an excellent way to quickly gauge nanoparticle uptake following exposure and confirms consumption. Based on the changes in average T_2 relaxation time, the 12 nm:5 kDa nanoparticles were the most impactful and were therefore selected for use in the remainder of this study.

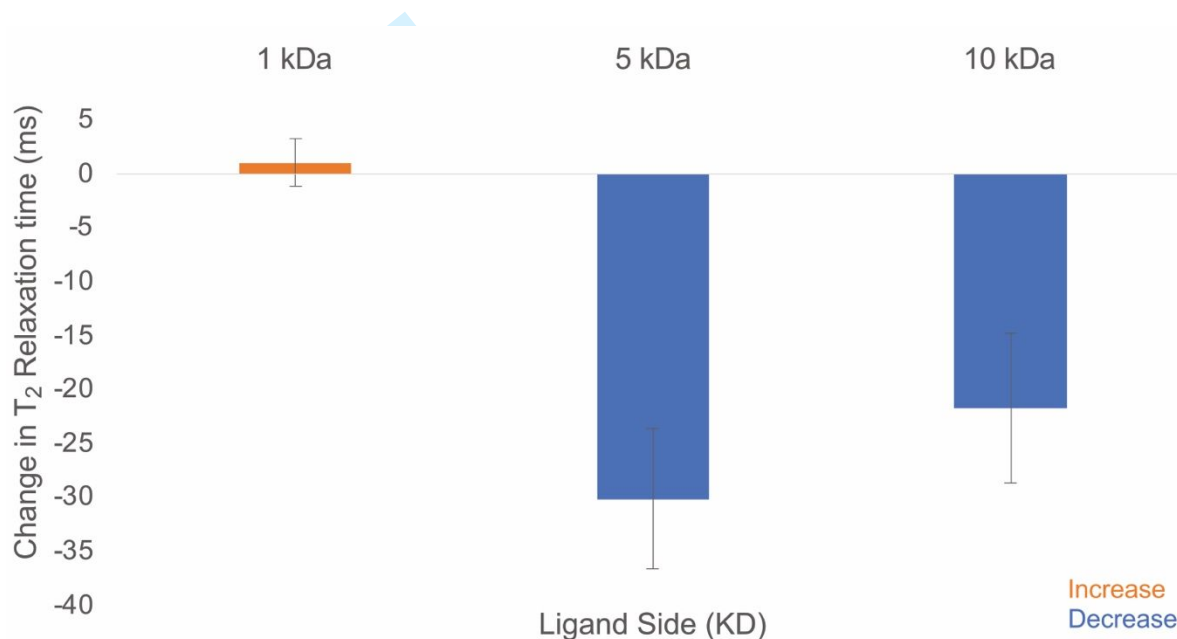


Figure 4. Changes in T_2 relaxation inside dead *Daphnia magna*. Control *Daphnia* were not exposed to nanoparticles and their T_2 relaxation was measured as an average of the whole organism. Relaxation of exposed organisms was then measured, and the change in the relaxation relative to the controls plotted. In the 1 kDa ligand there was no obvious decrease in the relaxation time (orange), indicating no uptake of nanoparticles, whereas in both 5 and 10 kDa there was a decrease. 12 nm:5 kDa nanoparticles were determined to be most impactful due to the highest average decrease in relaxation time (~30 ms) based on uptake and were chosen for further study. Each experiment was conducted in triplicate and error bars represent standard error in the measured changes.

T_1 Weighted Spectroscopy

While imaging can provide a physical overview of SPION locations, the impact of relaxation weighted spectroscopy on SPIONs can be useful in unravelling the chemistry, or the “what” with respect to binding, in the system. Due to their paramagnetic nature, SPIONs can be studied by relaxation weighted spectroscopy, which holds potential to elucidate the types of chemical structures within *Daphnia magna* they interact with. Having exploited the T_2 effect^[36] of SPIONs

in imaging experiments, here the T_1 capabilities are applied. Due to the overlap in the ^1H NMR of *Daphnia*, ^1H - ^{13}C HSQC is used to provide additional spectral dispersion to allow identification of chemical structures. To provide T_1 information, a 3rd dimension is acquired where a T_1 storage period is ramped via a delay list. After the processing the 3D cube contains a series of HSQC spectra which are progressively dampened via T_1 relaxation. To visualize the important differences in the data, a heat map in Figure 5 is used to show the changes in the relaxation times of each metabolite inside *Daphnia magna* relative to control organisms. Chemical shifts that are red have the largest changes in T_1 , as compared to control (SPION free), where beige shows little to no interaction.

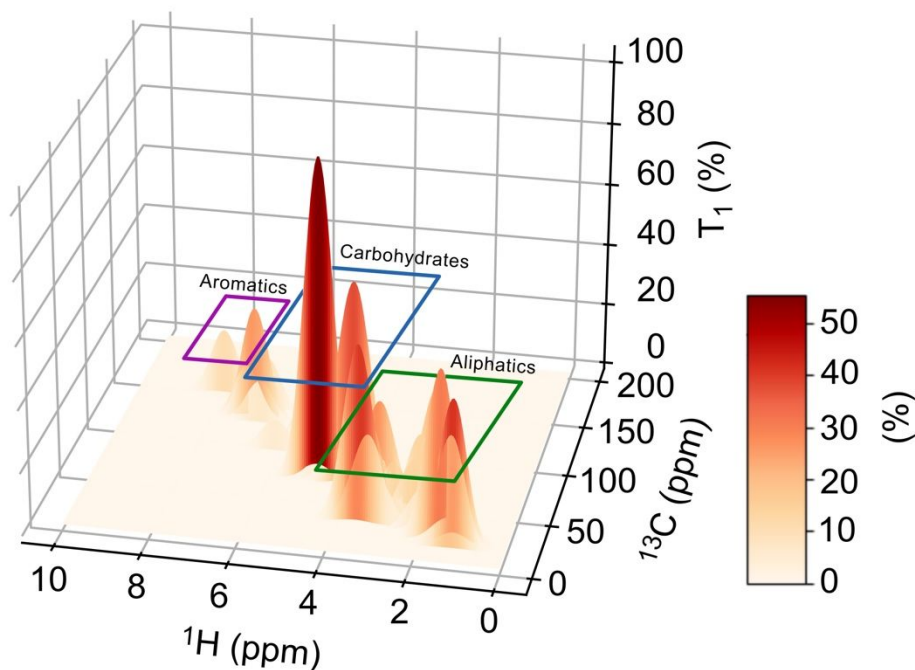


Figure 5. Changes in the T_1 relaxation, relative to the controls, inside *Daphnia magna* (dosed with 5kDa-grafted 12 nm SPIONs) as a heat map with specific regions highlighted of the intact, *ex-vivo* organism re-swollen and unwashed. Aliphatics and aromatics are boxed in green and purple respectively with most signals arising from amino acids, including alanine, asparagine, histidine, leucine, proline and tyrosine. This is most likely as a result of general protein binding. Carbohydrates are contained in the blue box, which is consistent with Chitin, the main component of the organism's carapace (shell).

In *in-vivo* ^1H NMR spectra there are three general δ areas, namely: aliphatics, carbohydrates, and aromatics, which can be seen in coloured boxes in Figure 5. Within the aliphatics and aromatics, the largest changes were present in the amino acid region from alanine, leucine, histidine, asparagine, proline, and tyrosine. Not all amino acids can be assigned due to spectral overlap but reduction in the T_1 time of a wide range of amino acids is generally consistent with protein binding. It is well documented that despite their great hydration and rapid dynamics PEG chains can interact with proteins in aqueous solution.^[37] Protein – PEG interactions could play an important role in SPION retention and could help explain the preferential uptake of the

1
2
3 5kDa/10kDa coated particles observed with imaging. As imaging supports the high
4 concentrations of SPIONs around the heart, it is possible that the SPIONs in the circulatory system
5 are interacting with hemolymph proteins. Such interactions are well documented when high
6 molecular weight PEG grafts are present.^[38]
7
8

9 However, the regions with the largest percent T_1 changes were the carbohydrates. These regions
10 most likely arise from chitin, which is the predominant structure in the carapace.^[39–41]
11 Interactions were not seen with the outside of the shell in imaging due to the washing step.
12 However, here the intact but dead organisms are re-swollen and unwashed, thus the reduction
13 in the T_1 times of chitin-like signals are consistent with the carapace playing an important role in
14 SPION binding in nature, as seen with other nanoparticles in the environment.^[9–11]
15 Unfortunately, it is not possible to determine the binding mechanism, but the fact that washing
16 removes the nanoparticles suggests the interaction is relatively weak, with one possibility being
17 that nanoparticles are able to be partially trapped in the relatively porous chitin structure.^[42]
18
19
20

21 Determining where nanoparticles bind is important to their potential uptake, retention, and
22 impact in the organisms. However, it provides little information as to the sub-lethal toxicity. To
23 determine how the organisms respond to the SPIONs presence, *in-vivo* metabolomics is highly
24 complementary.
25
26

27 *In-Vivo* Spectroscopy

28 Thus far, imaging has provided information on the physical location of SPIONs, and relaxation
29 weighted 2D has provided clues as to their molecular interactions. However, one missing aspect
30 is the toxic-mode-of-action of SPIONs, or in simple terms, “how” SPIONs are toxic. *In-vivo*
31 spectroscopy is ideal to address this gap. To our knowledge, nanoparticle impacts have not been
32 studied using *in-vivo* NMR in *Daphnia*, but previous *in-vitro* assays have shown a decrease in
33 energy creating metabolites, including glucose, glutamate, glutamine, tyrosine, histidine, and
34 ATP production as a mechanism to increase molting, a documented response of the organism to
35 the presence of externally interacting nanoparticles.^[10,11]
36
37
38
39

40 In the current study, organisms are first allowed to acclimatize to the conditions in the flow
41 system as per previous protocols^[43] without the presence of SPIONs. After 6 hours the SPIONs
42 are introduced and monitored for an additional 18 hours, resulting in a 24-hour total experiment
43 time. HSQC detection is used to provide spectral dispersion required for metabolite assignment.
44 All cross peaks were screened using manual peak-picking, and assignments were confirmed as
45 previously described.^[22] The metabolites with the most significant changes are plotted in Figure
46 6. As in previous reports, decreases in relative concentration of glycine, glutamine, and histidine
47 were seen. These are key metabolites related to increased energy demand and oxidative
48 stress.^[11,16] It has also been shown in previous work that the disturbance of nanoparticles
49 increased lactate because of anaerobic metabolism.^[11] However, similar trends were not seen
50 here, likely due to the low nanoparticle concentration. It is hypothesized that sustained exposure
51 would eventually cause a shift to anaerobic metabolism as energy stores are depleted, and food
52 and oxygen uptake slow due to aggregation of nanoparticles on the outside the organisms.
53
54
55
56
57
58
59
60

An additional metabolite methionine, not previously reported in nanoparticle studies on *Daphnia*, was seen to cycle with larger impact, relative to control organisms. Methionine is a key metabolite, which is replenished in the TCA cycle, indicating that energy production is being significantly impacted due to SPION exposure.^[17] This could be due to oxidative stress caused from a build-up of electrons in the electron transport chain due to the new energy requirements. The increased electrons create reactive oxygen species (ROS) in the organisms, which have been directly implicated in cell aging and death.^[10,44] L-glutathione was also measured to decrease relative to the control. This metabolite is used to help remove ROS by creating a protein which aids in their removal from the body.^[45] This decrease indicates that both processes mentioned above may be taking place simultaneously in the organism.

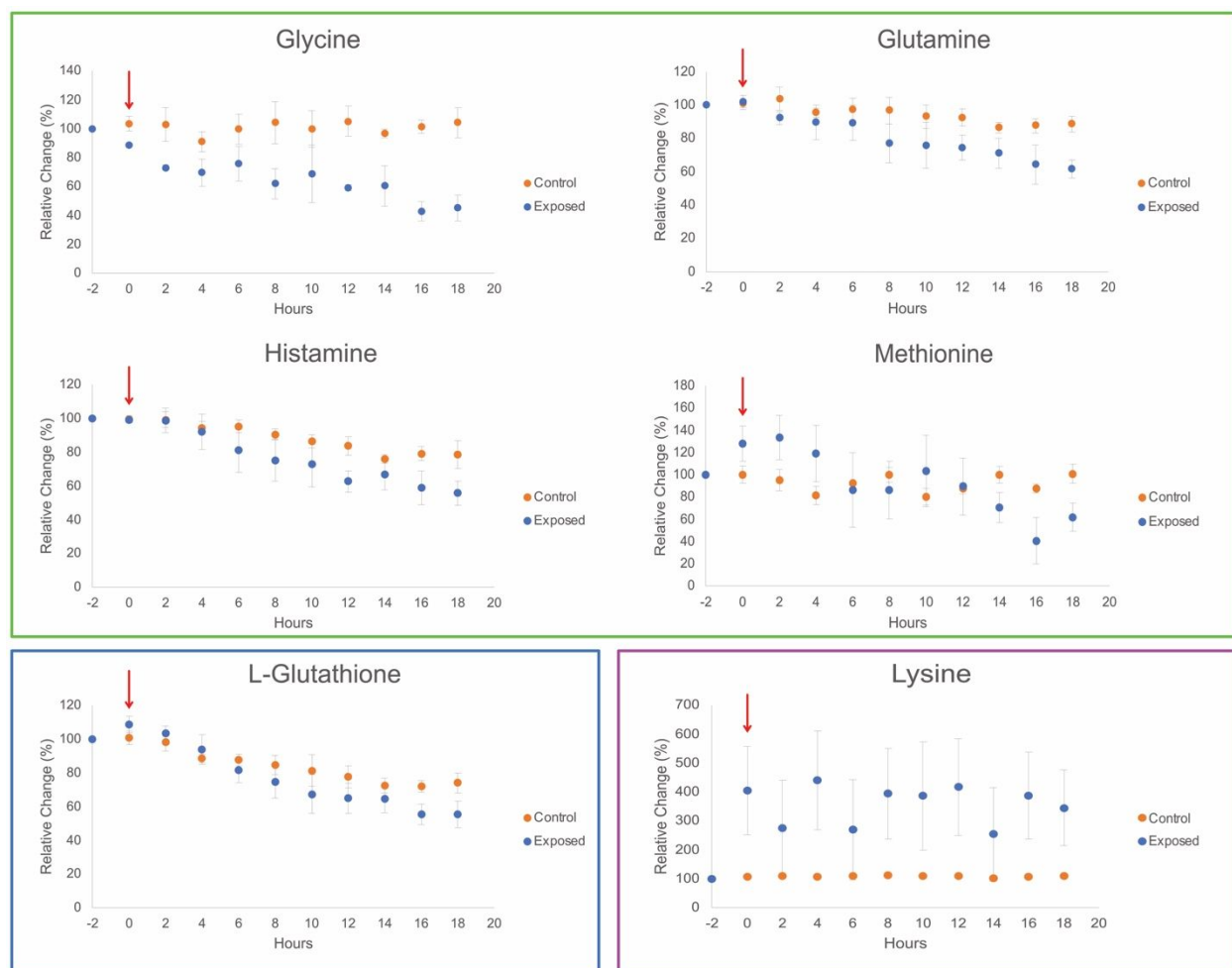


Figure 6. Metabolite responses in *Daphnia magna* due to nanoparticle exposure *in-vivo*. The upper green box shows the down regulation of metabolites resulting from increased energy metabolism, likely due to the nanoparticles both aggregating to the outside of the organisms resulting in increased molting requirements, and through consumption impacting the circulatory system. The lower left blue box indicates the down regulation of L-glutathione, an important metabolite in the removal of ROS. A decrease in this metabolite indicates it is likely being utilized to counteract ROS created from the increased energy requirements. Loss of this metabolite introduces DNA damage caused by cell aging and death. The lower right purple box indicates an increase in lysine. In each graph blue represents exposed *Daphnia*, and orange represents the control. Results are plotted as percent change relative to the first control point. The X-axis shows one point prior to exposure (-2 hours). Point 0 represents when SPIONs were exposed (also represented by a red arrow). Each experiment was conducted in triplicate and error bars represent standard error.

1
2
3
4 One additional component to note is lysine. Previous studies have indicated that lysine decreases
5 as a response to oxidative stress response,^[11] however, in this study it increased significantly in
6 the presence of SPIONs relative to the control. As can be seen in Figure 6 (purple box), the
7 response was quite variable and thus harder to quantify in the presence of the nanoparticles.
8 This may be because lysine is known to bind strongly to PEG.^[46,47] Historically, the combination
9 of PEG and lysine have been used to help keep biological implants from being rejected due to
10 their stability and ease of binding. This binding would impact the TCA pathway which has
11 potential impacts with respect to DNA repair and protein degradation due to oxidative
12 stress.^[11,48] These results indicate that even at sub-lethal concentrations, SPIONs cause a large
13 impact to *Daphnia magna* from which they may be unable to recover.
14
15
16
17

18 **Conclusion**

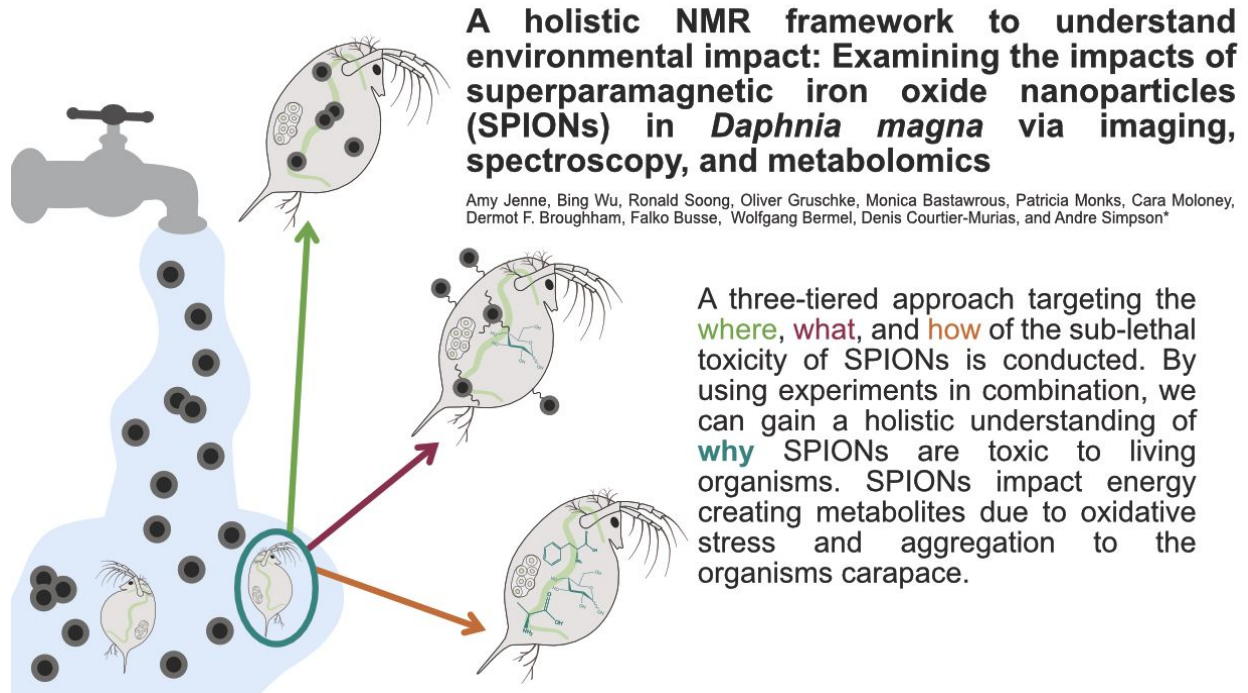
19 This research describes a three-pronged approach to examine toxicity in living organisms, which
20 provide holistic understanding of how contaminants interact in complex organisms. Using all
21 three NMR experiments together was critical to gain a complete understanding of the toxic-
22 mode-of-action, answering “why” SPIONs are toxic. Confirmation of SPION uptake was provided
23 by MRI, and accumulation in the area of the heart was consistent with SPIONs entering the
24 *Daphnia’s* hemolymph. Relaxation weighted spectroscopy supported two main “targets” of
25 interaction. One with the chitin in the carapace and the other with protein, likely within the
26 hemolymph. The organism’s response manifested as an increase in energy and oxidative stress
27 related metabolites. The results suggest that even at sub-lethal concentrations, SPIONs cause a
28 large negative impact to *Daphnia magna*. Continued study on the longer-term impacts of SPIONs
29 is recommended given the present environmental concentrations and projected future
30 increases. Combining different magnetic resonance techniques provides insight into any changes
31 in macroscopic structural characteristics and molecular processes induced by exposure to
32 SPIONs. Similar approaches may be of value for evaluating the impact of the wide range of
33 paramagnetic and ferromagnetic nanoparticles, and metal-organic complexes that are being
34 released into the environment.
35
36
37
38
39
40
41
42
43
44
45
46
47
48
49
50
51
52
53
54
55
56
57
58
59
60

Acknowledgements

We would like to thank the Natural Sciences and Engineering Research Council of Canada (NSERC) [Alliance (ALLRP 549399), Alliance (ALLRP 555452) and Discovery Programs (RGPIN-2019-04165)], the Centre national de la recherche scientifique (CNRS) PhD Mobility Funding Programme, the Canada Foundation for Innovation (CFI), the Ontario Ministry of Research and Innovation (MRI), the Krembil Foundation for providing funding, and the Government of Ontario for an Early Researcher Award.

- [1] D.L. Huber, *Small* **2005**, *1*, 482.
- [2] N. Wilson, *BioScience* **2018**, *68*(4), 241.
- [3] M. Bundschuh, J. Filser, S. Lüderwald, M.S. McKee, G. Metreveli, G.E. Schaumann, R. S. Wagner, *Environ. Sci. Eur.* **2018**, *30*(1), 6.
- [4] A.M. Gutierrez, T.D. Dziubla, J.Z. Hilt, *Rev. Environ. Health* **2017**, *32*(1-2), 111.
- [5] A. Amirshaghghi, Z. Cheng, L. Josephson, A. Tsourkas, in *Molecular Imaging: Principles and Practice*, 2nd Ed. (Eds.: B.D. Ross, S. Gambhir), Elsevier Inc., **2021**, pp. 679–98.
- [6] J. Matuszak, P. Dörfler, J. Zaloga, H. Unterweger, S. Lyer, B. Dietel, C. Alexiou, I. Chica, *Clin. Hemorheol. Microcirc.* **2015**, *61*(2), 259.
- [7] L.H. Reddy, J.L. Arias, J. Nicolas, P. Couvreur, *Chem. Rev.* **2012**, *112*(11), 5818.
- [8] N. Singh, G.J.S. Jenkins, R. Asadi, S.H. Doak, *Nano Rev.* **2010**, *1*, 5358.
- [9] A. Dabrunz, L. Duester, C. Prasse, F. Seitz, R. Rosenfeldt, C. Schilde, G.E. Schaumann, R. Schulz, *PLoS One* **2011**, *6*(5), e20112.
- [10] W. Wang, Y. Yang, L. Yang, T. Luan, L. Lin, *Ecotoxicol. Environ. Saf.* **2021**, *222*, 112491.
- [11] L.Z. Li, H. Wu, C. Ji, C.A.M. van Gestel, H.E. Allen, W.J.G.M. Peijnenburg, *Ecotoxicol. Environ. Saf.* **2015**, *119*, 66.
- [12] A. García, R. Espinosa, L. Delgado, E. Casals, E. González, V. Puentes, C. Barata, X. Font, A. Sánchez, *Desalination* **2011**, *269*, 136.
- [13] P.J. McDonald, J.P. Korb, J. Mitchell, L. Monteilhet, *Phys. Rev. E: Stat., Nonlinear, Soft Matter Phys.* **2005**, *72*(1), 011409.
- [14] M. van Landeghem, A. Haber, J.B.D. de Lacaillerie, B. BlüMich B, *Concepts Magn. Reson., Part A* **2010**, *36A*(3), 153.
- [15] B.P. Lankadurai, E.G. Nagato, M.J. Simpson, *Environ. Rev.* **2013**, *21*(3), 180.
- [16] M. Bastawrous, M. Tabatabaei-Anaraki, R. Soong, W. Bermel, M. Gundy, H. Boenisch, H. Heumann, A.J. Simpson, *Anal. Chim. Acta* **2020**, *1138*, 168.
- [17] A. Jenne, W. Bermel, C.A. Michal, O. Gruschke, R. Soong, R. Ghosh Biswas, M. Bastawrous, A.J. Simpson, *Angew. Chem. Int. Ed.* **2022**, *61*, e202110044; *Angew. Chem.* **2022**, *134*(19), e202110044.
- [18] M.T. Anaraki, D. Lane, M. Bastawrous, A. Jenne, A.J. Simpson, in *NMR-Based Metabolomics. Methods Molecular Biology*, Vol. 2037 (Eds.: G. Gowda, D. Raftery), Humana, New York, **2019**, pp. 395–409.
- [19] R. Soong, Y. Liaghati Mobarhan, M. Tabatabaei, M. Bastawrous, R. Ghosh Biswas, M. Simpson, A.J. *Magn. Reson. Chem.* **2020**, *58*(5), 411.
- [20] A. Jenne, R. Soong, W. Bermel, N. Sharma, A. Masi, M. Tabatabaei-Anaraki, A.J. Simpson, *Faraday Discuss.* **2019**, *218*, 372.

- 1
2
3 [21] D. Lane, et al., *ACS Omega* **2019**, *4*, 9017.
4 [22] M. Tabatabaei Anaraki, et al., *Anal. Chem.* **2018**, *90*(13), 7912.
5 [23] N. Pinna, S. Grancharov, P. Beato, P. Bonville, M. Antonietti, M. Niederberger, *Chem.*
6 *Mater.* **2005**, *17*(11), 3044.
7 [24] T. Ninjbadgar, D.F. Brougham, *Adv. Funct. Mater.* **2011**, *21*, 4769.
8 [25] R. Soong, E. Nagato, A. Sutrisno, B. Fortier-McGill, M. Akhter, S. Schmidt, H. Heumann,
9 A.J. Simpson, *Magn. Reson. Chem.* **2015**, *53*, 774.
10 [26] E.G. Nagato, B.P. Lankadurai, R. Soong, A.J. Simpson, M.J. Simpson, *Magn. Reson. Chem.*
11 **2015**, *53*, 745.
12 [27] D. Lane, et al., *Anal. Chem.* **2019**, *91*(23), 15000.
13 [28] G.C. Woods, M.J. Simpson, P.J. Koerner, A. Napoli, A.J. Simpson AJ, *Environ. Sci. Technol.*
14 **2011**, *45*(9), 3880.
15 [29] J.J. Ellinger, R.A. Chylla, E.L. Ulrich, J.L. Markley, *Curr. Metabolomics* **2013**, *1*(1), 28.
16 [30] M. Gophen, W. Geller, *Oecologia* **1984**, *64*, 408.
17 [31] W. Geller, H. Müller, *Oecologia* **1981**, *49*, 316.
18 [32] G. Liu, J. Gao, H. Ai, X. Chen, *Small* **2013**, *9*, 1533.
19 [33] P.K. Menon, A. Sharma, J.v. Lafuente, D.F. Muresanu, Z.P. Aguilar, Y.A. Wang, R. Patnaik,
20 H. Mössler, H.S. Sharma, *Int. Rev. Neurobiol.* **2017**, *137*, 47.
21 [34] J.K Stolarczyk, A. Deak, D.F Brougham, *Adv. Mater.* **2016**, *28*, 5764.
22 [35] R.D. Majumdar, M. Akhter, B. Fortier-McGill, R. Soong, Y. Liaghati-Mobarhan, A.J.
23 Simpson, M. Spraul, S. Schmidt, H. Heumann, *eMagRes* **2017**, *6*, 133.
24 [36] A. Alipour, Z. Soran-Erdem, M. Utkur, V.K. Sharma, O. Algin, E.U. Saritas, H.G. Demir,
25 *Magn. Reson. Imaging* **2018**, *49*, 16.
26 [37] J. Wu, C. Zhao, W. Lin, R. Hu, Q Wang, H. Chen, L. Li, S. Chen, J. Zheng, *J. Mater. Chem. B*
27 **2014**, *2*, 2983.
28 [38] J.J. Lai, H.Y. Yan, Y. Liu, Y. Huang, *Chin. J. Polym. Sci.* **2015**, *33*(10), 1373.
29 [39] M. Kaya, I. Sargin, K.Ö. Tozak, T. Baran, S. Erdogan, G. Sezen, *Int. J. Biol. Macromol.*
30 **2013**, *61*, 459.
31 [40] M.R Kasaai, *Carbohydr. Polym.* **2010**, *79*(4), 801.
32 [41] P. Gonil, W. Sajomsang, *Int. J. Biol. Macromol.* **2012**, *51*(4), 514.
33 [42] F. Hou, D. Wang, X. Ma, L. Fan, T. Ding, X Ye, D. Liu, *Ultrason. Sonochem.* **2021**, *70*,
34 105327.
35 [43] M. Tabatabaei Anaraki, M.J. Simpson, A.J Simpson, *Magn. Reson. Chem.* **2018**, *56*(11),
36 1117.
37 [44] D. Ren, Y. Li, Y. Xue, X Tang, L. Yong, Y. Li, *NanoImpact* **2021**, *24*, 100360.
38 [45] K. Lyu, L. Gu, B. Li, Y. Lu, C. Wu, H. Guan, Z. Yang, *Harmful Algae* **2016**, *56*, 1.
39 [46] D. Li, H. Chen, W. Glenn McClung, J.L Brash, *Acta Biomater.* **2009**, *5*, 1864.
40 [47] C.C. Lee, Y.C. Su, T.P. Ko, L.L. Lin, C.Y. Yang, S.S.C Chang, S.R. Rofler, A.H.J. Wang, *J.*
41 *Biomed. Sci.* **2020**, *27*(12).
42 [48] M. Kariuki, E. Nagato, B. Lankadurai, A. Simpson, M. Simpson, *Metabolites* **2017**, *7*(2),
43 15.
44
45
46
47
48
49
50
51
52
53
54
55
56
57
58
59
60



Peer Review